tactoRing: A Skin-Drag Discrete Display

Seungwoo Je[1] **Brendan Rooney**[2] **Liwei Chan**[3] **Andrea Bianchi**[1]

[1]Department of Industrial Design, KAIST, Daejeon, Korea
{Seungwoo_je, andrea}@kaist.ac.kr

[2]Department of Mathematical Sciences, KAIST, Daejeon, Korea
brooney@kaist.ac.kr

[3]Computer Science, National Chiao Tung University, Hsinchu, Taiwan
liweichan @cs.nctu.edu.tw

ABSTRACT
Smart rings are an emerging wearable technology particularly suitable for discrete notifications based on haptic cues. Previous work mostly focused on tactile actuators that stimulate only specific skin receptors on the finger, resulting in limited information expressiveness. We propose *tactoRing*, a novel tactile display that, by dragging a small tactor on the skin around the finger, excites multiple skin areas resulting in more accurate cue recognition. In this paper we present the hardware and a perception study to understand the ability of users to recognize eight distinct points around the finger. Moreover, we show two different techniques to encode information through skin-dragging motion with accuracy up to 94%. We finally showcase a set of applications that, by combining sequences of tactile stimuli, achieve higher expressiveness than prior methods.

AUTHOR KEYWORDS
Haptics; wearable; ring; eyes-free; skin-drag.

ACM Classification Keywords
H.5.2. [Information interfaces and presentation]: User Interfaces – Haptic I/O

INTRODUCTION
Smart rings are becoming more popular, receiving both commercial endorsement and attention from researchers [29]. Like other wearable devices, they benefit from the social acceptability of traditional jewelry [22], but also from direct contact with the finger skin. These properties make them particularly suitable for always-available input interactions [1, 5, 18, 24, 35], and rich but subtle notifications [21, 28]. It is therefore unsurprising that researchers have explored a variety of notification modalities for smart rings and similar finger augmentation devices, including: light [16]; small displays [30]; sound [28]; and, in particular, tactile feedback. Several types of tactile feedback have been considered, including: vibration patterns [3, 12, 21]; pressure and shear [36]; force [15, 19, 26]; and, poke and thermal [28].

CHI 2017, May 06-11, 2017, Denver, CO, USA
 ISBN 978-1-4503-4655-9/17/05…$15.00
DOI: http://dx.doi.org/10.1145/3025453.3025703

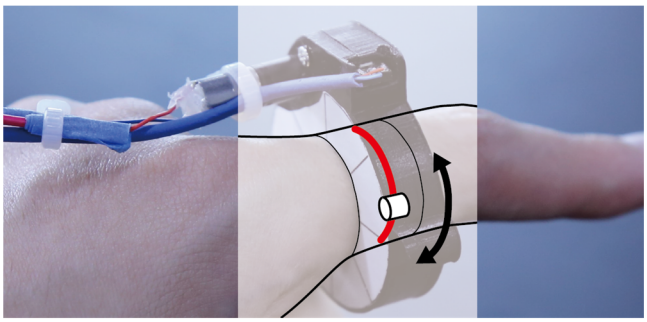

Figure 1. *tactoRing* contains a small movable skin-drag tactor that can rotate around the finger. Motion is indicated by the black arrow, and the dragging surface area in red.

However, while tactile notifications have the benefit of not requiring constant attention from users, and support eyes-free interactions, the expressiveness and the amount of information that can be clearly communicated to users through the haptic channel using currently available finger wearable devices is quite limited. In fact, most of these devices operate by exciting only a small set of tactile skin receptors [13, 36]. They fail to exploit the spatial resolution of the finger skin, which is capable of disambiguating points as close as 2-5mm [14, 33].

In this paper we present *tactoRing*, a novel haptic ring that excites the user's skin by dragging a small movable tactor (i.e., a small tactile actuator, such as a pin) around the finger. By simultaneously stimulating the Merkel cells on the epidermis (SA1) through pressure, and the Meissner corpuscles (RA1) and the Ruffini's endings (SA2) in the dermis through stretching the skin and low frequency vibrations (e.g., rubbing) [14], we are able to achieve higher discrete spatial resolution on the finger and convey richer and more expressive messages to users than traditional methods.

This paper describes the *tactoRing* prototype in detail, and demonstrates its accuracy with a series of user studies. Specifically, we investigated the capability of users to perceive the movable tactor and discern its dragging motion to different locations around the finger. To overcome low spatial resolution, we present two different interaction techniques based on skin dragging (*DoublePoint* and *VirtualPoint*) and demonstrate, with a study, that they are suitable for accurate identification of eight unique targets around the finger. Finally, we instantiate concrete examples of usage for the presented techniques in four applications, and indicate possible future research directions.

RELATED WORK

Haptic output through finger augmentation has been explored for applications such as: manipulating virtual objects [7, 19, 36]; pointing devices [6, 18]; delivering eyes-free notifications [21, 28]; intimate communications [25]; accessibility [10]; and, guiding fingers [11]. While multi-finger augmentation with several degrees of freedom is possible, and is much studied [e.g., 9, 15], this approach is infeasible for wearable devices. Therefore, this paper focuses on a single-point actuation method. The rest of the related work covers only techniques that provide temporal and spatial haptic output through finger augmentation.

Temporal and Spatial Haptic Output on the Finger

Early examples of temporal encoding of tactile feedback adopted "Morse-like" vibration patterns using a single actuator [31]. This model was later generalized in the concept of *Tactons* [3], an identifiable set of tactile icons that can be created with different vibration parameters such as frequency, amplitude, duration, and rhythm. However, temporal signals are more difficult to interpret and memorize than spatial ones. Utilizing the spatial resolution of the finger's skin, Khurelbaatar et al. [17] presented an electrode-tactile grid placed on the back of a touchscreen that can display different tactile shapes on a single fingertip. *NailTactors* [12] instruments a nail with an array of vibration motors, allowing the finger to perceive directional and numerical cues through spatial encoding of vibrations.

Haptic Cues that Poke, Stretch, Pull and Drag the Skin

Beyond temporal and spatial encoding of tactile feedback, recent research explored novel haptic modalities by applying tangential forces on the skin to expand haptic expressiveness while improving the capability of skin recognition. Tapping and rubbing skin as intimate haptic cues were first proposed by Li et al. [20]. *NotiRing* [28] presented a user study comparing taps against other types of haptic notifications (vibration and thermal). The result echoed Li's finding that tapping feels natural and simulates an affective human touch. Skin stretching and pulling (i.e., rubbing) were also explored. Prior work [2, 4] demonstrated that stretching and pulling provide more accurate directions than vibrotatctile stimuli because they excite a wider range of skin receptors.

Highly relevant work about lateral skin stretching on the fingerpad was proposed by Provancher et al. [26]. Results show that even small amounts of tangential skin stretching (0.25-0.75 mm) can greatly increase the perception of friction, and that this technique is suitable for communicating directional cues in four directions [8]. This work was further extended leading to the development of complex non-wearable devices for 5-degree-of-freedom directional cue communication [9] and a graspable 3-degree-of-freedom device capable of rendering both normal and tangential skin deformation [27]. Finally, Ion et al. [13] combined the idea of skin stretching with that of skin dragging, and proposed a wearable skin-drag display that draws spatial cues on the wrist using a dragging tactor.

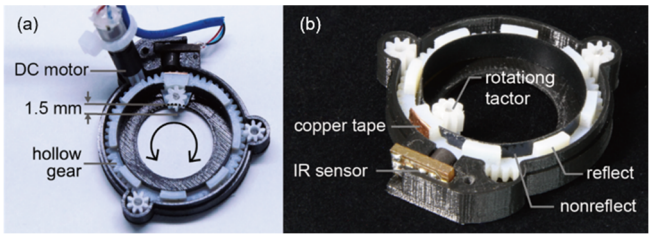

Figure 2. Working principles and detail description of the components of *tactoRing*.

Our work differs from the work on skin stretching by Provancher [26] and the work on wrist-wearable dragging display by Ion [13], because of the wearable form factor of the proposed skin-dragging display (specifically, a ring), and because of the type of haptic stimulus generated. In fact, we mainly focus on dragging on a continuous non-flat contact surface. Though skin dragging shares common elements with stretching, as explained in [13], these interactions are different for both the number and the type of mechanoreceptors involved, and the size and geometry of the area. We are not aware of any prior work that presented high-resolution spatial haptic encoding of discrete information on the finger. In this work, we introduce a haptic ring based on the one-dimensional (1-D) skin-drag movement of a small tactor, and present evidence of its high accuracy in discerning distinct spatial dragging locations around the finger.

SKIN-DRAGGING RING

tactoRing is a novel haptic ring which works by mechanically dragging a small tactor in a 1-D path around the user's finger (Figure 1). Like previous skin-dragging interfaces designed for different body parts [4, 13], *tactoRing* stimulates both slow- and fast-adapting mechanoreceptors on the epidermis and the dermis (SA1, SA2, RA1). As a consequence, the user can clearly perceive a small localized pressure applied to the skin when the tactor is dragged, and therefore determine its locations.

Prototype

tactoRing (Figure 2) is based on a system of spur gears (0.5 module) and a small DC motor (LCP06-A03V-0136 with torque 120gf-cm, 25 mA at 3V) capable of spinning a tactor along the inner face of the ring. An infrared (IR) sensor (SG-2BC) mounted on the bridge of the ring is used to track and encode the relative motion of the gears, and to infer the tactor location around the finger. All components are housed in an external case which was 3-D printed using PolyLactic Acid (PLA). The case has a diameter of 35mm, and the finger hole has a diameter customizable up to 20.68mm (US size 11). Inside the ring, three spur gears (8 teeth, 5mm face width) are positioned 120° apart and surround a larger hollow gear (60 teeth, 2.5mm face width) which was custom designed and 3-D printed with *VeroWhite* material. The hollow gear profile has eight reflective and non-reflective regions used by the IR sensor to distinguish eight locations 45° apart.

The tactor is placed on the inner side of the hollow gear, mounted on a flat extrusion. When the gear moves, the tactor also moves. The tactor is also shaped as a gear that can rotate on itself, and it is placed in such way that it protrudes only 1.5mm from the case toward the inside of the ring. The rationale for the choice of a gear-shaped rotating tactor is that the finger is not perfectly cylindrical and the distribution of tissues is uneven, so the tactor needs to adapt to different surfaces. Empirically we found that a small fixed tactor (<3mm) is not equally perceived around the finger, and a longer tactor can be entangled in the skin generating a stalling torque. Therefore, we adopted the design of a rotating gear where each tooth of the gear acts as a pin when in contact with the skin, and the rotation of the gear minimizes friction caused during dragging. Since the spatial resolution on the proximal phalanx (the part of the fingers closest to the metacarpus) is 5mm, the adjacent teeth of the tactors are perceived as a single entity [14, 33].

The ring is wired to an external electronic board used for driving the motor, and an Arduino UNO, connected to a PC, for reading the sensor data and controlling the tactor location. Analog readings from the IR sensor are sampled on the Arduino controller at 10 KHz, then filtered using a low-pass filter with 15 Hz cutoff frequency (Hamming window, order 100). By physically applying reflective copper on the region of the hollow that corresponds to the tactor location, we are able to identify when the tactor is placed in front of the IR sensor (this region corresponds to 0° and we refer to it as *home*). The remaining reflective and non-reflective regions of the gear are identified using adaptive thresholds that are dynamically adjusted at run-time using a moving average with a window of 800 samples.

The PC software is written in Java and consists of a graphical interface containing several controllers for changing the ring behavior. Using this software, it is possible to change the motor speed (160 rpm, 180 rpm, and 200 rpm) and direction (left, right). It is also possible to choose a target dragging location (or sequences of locations) among the eight designated regions, and to recalibrate the ring by moving the tactor to *home*. Finally, the PC software enables external devices, such as tablets and mobile devices, to wirelessly connect and issue commands to the ring using the Open Sound Control (OSC) protocol.

Prototype Validation

Since *tactoRing* works by mechanically stimulating the skin around the finger with a movable part, it is necessary that the tactor is permanently in contact with the user's skin. An oversized ring would result in imprecise perception, while an undersized ring could obstruct the motion of the tactor. Accordingly, the ring size should be appropriate for the user who wears it. We therefore built two rings with different sizes. Because we could not find suitable data in the ergonomic database for the size of the proximal phalanx of the index finger, we collected finger sizes for 48 participants (22 female) from our institution and chose the two most common sizes. We then built a large ring (covering US size 10-11) and small one (US size 7-8), respectively suitable for the 35% and 31% of the population that we sampled.

We then recruited 20 participants (10 for each ring size, 10 females, mean age 25.4, SD 2.6) for a pilot study aimed to test whether the tactor movement was accurate and reliable across finger sizes. In the pilot, no user input was required. Instead, users simply wore the ring of their size while our software instructed the tactor to follow 10 randomized motion sequences. Each sequence consisted of movements to 40 locations (5 for each of the 8 target locations, every 45°) with the motor spinning at maximum speed (200 rpm). At the end of every sequence we manually inspected the actual tactor location and checked whether it matched with the location reported by the software. This is a simple way to verify whether any obstruction altered the tactor motion. The pilot took about 15 minutes per participant and in total we collected data for 200 sequences of motions (100 for each ring size). The rings performed with overall accuracy of 97.5% (small: 97%, large: 98%) with a total of 5 errors (each distance one from the expected target). We concluded that the ring performance was sufficient for further user studies and, to avoid errors propagating through an entire experimental session, we modified the controlling software to perform an implicit recalibration anytime the tactor was moved to *home*.

EVALUATION OF TARGET RECOGNITION

We conducted a user study to investigate the ability of users to distinguish among different tactor dragging locations. In this experiment, the term *location* is used to identify not a single-point stimulation around the finger, but a dragging motion pattern, which ends in a specific target point. We tested three configurations, *complete*, *square* and *diamond* (Figure 3). The *complete* configuration has eight target locations spaced 45° apart, starting from 0°; the *square* and *diamond* configurations each have four target locations spaced 90° apart, starting respectively from 45° and 0°. Clearly, the *square* and *diamond* configurations together form the *complete* configuration. Considering the high spatial resolution of the skin on the proximal phalanx (5 mm), the size of the tactor (5mm), and the diameter of our rings (57.2mm and 64.9mm), we formed the hypothesis that all three configurations result to similar recognition performance with comparable error rates, input time, and cognitive workload.

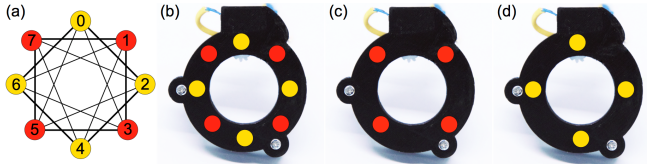

Figure 3. The targets modeled as a graph (a); the *complete* (b), *square* (c), and *diamond* (d) configurations of targets.

We recruited 12 volunteers (5 female) from our institution, aged 22-30 (M: 24.2, SD: 2.3) with finger size 8 or 11. Four participants reported familiarity with haptic interfaces and wearable devices, and two regularly wear a ring. None had prior experience with smart rings. Participants were compensated with 10 USD in local currency.

Following a repeated measures design, participants tested each configuration in a fully balanced Latin square order. In each configuration users wore a ring on the index of the left hand (Figure 4.a), and completed a series of selection trials with randomized target locations (see next section for details) using their right hand. In each trial, the tactor moved in a specific target location, using the shortest path, and stopped. After two seconds, users could select the perceived location on a graphical interface with the available options for the current configuration. This visual interface was displayed on a tablet (Figure 4.b) and wirelessly synchronized with the ring software. The tablet also provided auditory feedback during an initial training phase, using beeps to indicate hits and buzzes to indicate misses.

In total, each participant entered 240 trials for the *complete* 8-target configuration (30 repetitions per target); of which the first 80 trials (10 repetitions) were considered as training and discarded from the analysis. Similarly, for each of the two 4-targets configurations, users entered 120 trials; 40 of which discarded as training (10 repetitions). In total we collected 1920 valid trials (8 targets x 20 repetitions x 12 participants) for the *complete* configuration, and 960 trials (4 targets x 20 repetitions x 12 participants) for each of the *square* and *diamond* configurations. Finally, for each configuration users completed a NASA TLX questionnaire to measure cognitive workload.

Trials Randomization

In this section we describe the trial randomization method for the *complete* configuration; the other two configurations were handled analogously. The objective is to generate a sequence of randomized trials with eight target locations, each repeated exactly 30 times, that are not easy to guess (in other words, the information leakage from the skin-dragging motion of the tactor should be minimized). Therefore, we required consecutive trials of the experiments to be always at a fixed distance of either 2 or 3 target locations. That is because repeated positions in consecutive trials would be trivial to identify, and positions adjacent, or antipodal, to the current tactor location could be easily inferred from the duration of the dragging motion.

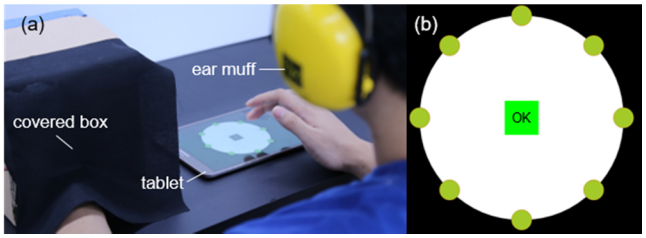

Figure 4. The experimental setup (a) and an example of GUI used by the participants for the target selection task.

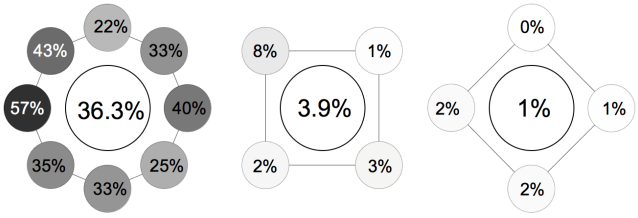

Figure 5. Target error rates for each configuration. The average error rate is displayed in the center of each figure.

Although it is easy to generate a random sequence of target positions that satisfy either the distance constraint, or the frequency constraint, doing both simultaneously is a difficult task. Specifically, this problem is equivalent to finding a Hamilton path (a path that visits every vertex exactly once [34]) in a graph with 240 vertices and 14,400 edges. Finding a Hamilton path is known to be a NP-complete problem [32], and our input graph is too large to generate valid random sequences in a reasonable time. Therefore, we used an alternative method that generates sequences of targets by combining subsequences obtained from the Hamilton cycles of the small graph in Figure 3.a. First, we enumerated the Hamilton cycles in that graph using brute force. From these we obtained 56 sequences of length 8 starting at the *home* location. We then concatenated 30 of these, chosen uniformly at random, and cyclically permuted the resulting sequences to randomize their starting positions (the first trial of the experiment). The resulting sequence satisfies our restrictions.

Results and Findings

Results were analyzed using one-way ANOVA tests followed by Bonferroni correction post-hoc analysis with α=0.05. Sphericity was assessed with Mauchley's test, and, if violated, Greenhouse-Geisser corrections were employed. Error rates in the *complete*, *square* and *diamond* configurations were respectively 36.3%, 3.9% and 1% (Figure 5). Specifically, in the *complete* configuration participants made on average 58 errors (SD: 28), of which 92% consisted of *1-errors* (i.e., selections one location away from the target). The *square* configuration resulted with an average of 3.1 errors (SD: 4.9), 97% of which were *1-errors*, and the *diamond* configuration resulted in an average of 0.8 errors (SD: 2.3), 80% of which were *1-errors*. Error rates

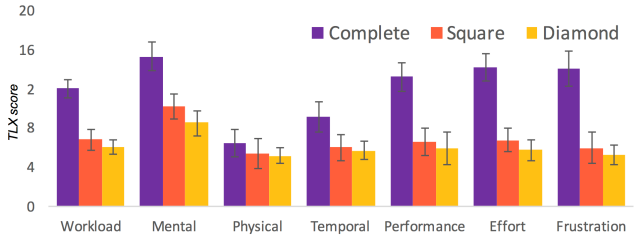

Figure 6. The results for the cognitive load based on the NASA TLX questionnaire. The vertical axis indicates the TLX score.

were tested statistically significant across interfaces ($F_{(1.13,12.4)}$=38.2, p<0.01, η^2_p=0.39) with the *complete* configuration performing worse than the others (p<0.01). Also the cognitive workload measures from the TLX (Figure 6) were statistically different ($F_{(2,22)}$=37.6, p<0.01, η^2_p=0.77) with the *complete* configuration performing worse than the others (p<0.01). The average input time for the *complete*, *square* and *diamond* configurations were respectively 1.2s (SD: 0.3), 1s (SD: 0.2), and 1s (SD: 0.3). We found statistical differences ($F_{(2,22)}$=7.18, p<0.01, η^2_p=0.39), but only the *complete* and *diamond* comparison was significant (p<0.01).

Our main hypothesis was that the three interfaces would perform similarly, regardless the number and location of the targets, simply because the spatial resolution of the skin on the finger is higher than the size of tactor utilized. We reject such hypothesis, as we observed that the *complete* configuration performed significantly worse than the other two. In fact, both *square* and *diamond* configurations had an accuracy of over 96%, but the *complete* configuration achieved only 63%, demonstrating that selecting a correct location out of eight targets was challenging. This result is corroborated by the TLX data about the cognitive workload, and by the post-hoc informal interviews we had with the participants (all participants agreed that the *complete* configuration was the most difficult). By comparing the differences between configurations we can also conclude that the overall accuracy did not depend on the target locations, but rather on their density. If specific parts of the fingers had lower sensitivity, we should have reported low performance for specific targets across configurations, but that did not happen. Finally, the fact that the majority of errors (80%-97%) were *1-errors*, further demonstrates that accuracy depended on the density rather than the location of the target locations around the finger.

NEW TECHNIQUES FOR TARGET SELECTION

From the previous study we concluded that identifying eight dragging locations around the finger is a difficult and error-prone task. In this section, we present two different interaction techniques that, by utilizing skin-dragging motion, allow users to correctly identify the same eight target locations from the previous study with better performance. These techniques use a pair of motions to represent a single target location. This introduces a second point that acts as a reference for the desired target. Our hypothesis is that users will be able to better identify the same targets that led to poor recognition rate in the previous study. The two techniques we present are named *DoublePoint* and *VirtualPoint* (Figure 7).

With *DoublePoint*, a target is represented by a motion pattern with a sequence of dragging motions starting from 0° and with the second motion spanning exactly 45°. The two motions are separated by a 200ms pause and can be either to the left or the right. For example, the target number 3 (135°) is encoded as the motion 0° ➔ 90° pause 90° ➔ 135°, while the target 1 (45°) is encoded as 0° ➔ 90° pause 90° ➔ 45° (➔ and ➔ meaning right and left movements). Figure 7-left shows the motion encodings for each target using the *DoublePoint* encoding scheme.

With *VirtualPoint* (Figure 7-right), a target is still identified by two distinct drag motions starting from 0° and separated by a 200ms pause, but a target is described as the middle point between the locations of the first and second stops. For example, target 3 is encoded as the motion 0° ➔ 90° pause 90° ➔ 180°, because the middle point between 90° and 180° is 135°. Similarly, target 1 can be described with the motion 0° ➔ 90° pause 90° ➔ 0°, resulting in 45°. *VirtualPoint*, differently from *DoublePoint*, encodes any target only using the four cardinal points (0°, 90°, 180°, 270°). In the previous study, these proved to be well recognized by all the users.

EVALUATION OF DOUBLEPOINT AND VIRTUALPOINT

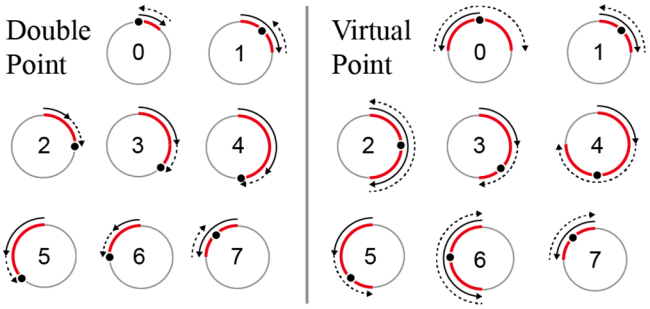

Figure 7. Selections using *DoublePoint* (a) and *VirtualPoint* (b). Destination targets are indicated with a black dot, motions with arrows (the second motion is dotted). The skin area stimulated by the dragging motion is highlighted in red.

To validate our design, we conducted a second user study similar to the previous one. We recruited again from our institution 12 participants (5 female), aged 22 to 26 (M: 23.5, SD: 1.1) with ring size 8 or 11. Following a repeated measure design, every participant tested the *DoublePoint* and *VirtualPoint* interfaces in balanced order, then completed a NASA TLX questionnaire. Each interface was tested for 240 trials (30 repetitions x 8 targets), of which the first 80 (10 repetitions) were discarded as training. During the training phase participants received an auditory feedback and could consult a drawing of the motions as in Figure 7. Finally, unlike the previous experiment, all motion sequences started from 0°. So after each input trial, the system automatically

Figure 8. *DoublePoint* and *VirtualPoint* performance for input time, error rate, and cognitive workload measured with a TLX.

placed the tactor at *home*. Participants were compensated 10 USD in local currency.

Results and Findings

Results were analyzed using a paired t-test with α=0.05. Average input times, number of errors, and cognitive workload are reported in Figure 8, and all revealed statistical differences. Input with *DoublePoint* was significantly faster ($t_{(11)}$=2.22, p<0.05) than with *VirtualPoint*, but was also more error prone ($t_{(11)}$=4.5, p<0.01) and cognitively difficult ($t_{(11)}$=2.3 p<0.05). Specifically, the *DoublePoint* error rate (18%) is about three times larger than that of *VirtualPoint* (5%). Confusion matrices and error rates for each motion sequence are indicated in Figure 9. For *DoublePoint*, clearly the targets 2-3-4 and 5-6, were confused with each other because of the similarities in the motion sequences. Finally, the error rate for *1-errors* was 68% for *DoublePoint* and only 48% for *VirtualPoint*.

DISCUSSION AND EXAMPLE APPLICATIONS

The *DoublePoint* and *VirtualPoint* selection techniques presented in the previous section achieve, in two different ways, the same objective: they allow users to disambiguate eight distinct point around the finger using the skin-dragging

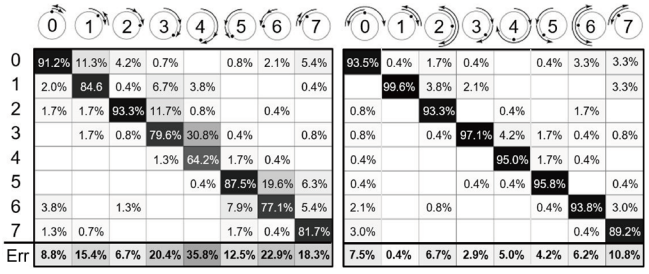

Figure 9. Confusion matrices for the *DoublePoint* (left) and *VirtualPoint* (right) techniques. Columns represent challenges and rows the participants' input.

motion of a tactor. Despite the differences in performance, it is clear that both techniques resulted in more accurate selections than absolute targeting of eight locations, as in the first experiment (error rates of 18% and 5% vs. 36% of the complete configuration). Specifically, identifying a single point though a pair of motions was perceived as easier to distinguish than static spatial recognition, because the dragging motion offered a clearly distinguishable reference point for comparison. This result is also aligned with past findings [23] which indicated that cutaneous spatial acuity is better for dynamic rather than static stimuli. Also, as an immediate result, the number of *1-errors* was greatly reduced from the previous experiment. Overall, the accuracy of 94% found in *VirtualPoint* demonstrates the feasibility of our approach as an alternative to vibrotactile encodings [3, 12] for the communication of distinguishable haptic cues.

In terms of differences between the two approaches, *VirtualPoint* is arguably cognitively more demanding (e.g., it requires more training) than *DoublePoint*, but interestingly it is easier at the physiological perception level. In fact, with *VirtualPoint* users only needed to distinguish among four cardinal points, instead of the eight distinct dragging locations necessary for the *DoublePoint*. The trade-off between cognitive load and perception clearly emerged in this experiment, showing that for simple tasks such as recognizing pairs of motions as in the *VirtualPoint* technique, higher accuracy can be achieved by simplifying the perception task at the expense of slightly higher cognitive load.

Finally, we argue that *DoublePoint* could perform better if the motion sequences were redesigned to be less ambiguous. For example, both targets 3 and 4 consist of two long motions on the right, followed by a short motion in the same direction. We believe that by changing some of these encodings, we could achieve better performance (for example, motion 3 could be encoded as 0° ➔ 180° pause 180° ➔ 135°). Future work will investigate possible different motion encodings and their accuracy.

Applications

We present four possible practical applications for *tactoRing* and the targeting techniques described in this paper. In these examples, the haptic feedback can be composed of single motions, dragging selections using the *VirtualPoint* and *DoublePoint* techniques, or even sequences of these motions for more expressiveness.

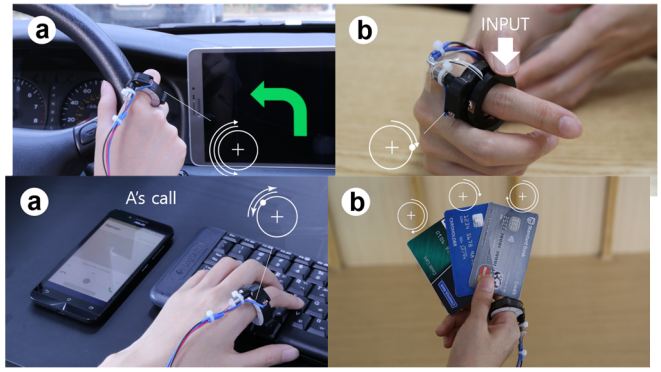

Figure 10. Two applications demonstrating *tactoRing* use for eyes-free delivery of qualitative and quantitative information.

We developed four proof-of-concept applications using the existing platform. The first two applications are examples of how different motion targets on the ring can be associated with different meaning. As in Figure 10.a, we developed an Android application that simulates phone calls, incoming messages and calendar events. When any of these events happen, a notification is initiated by moving the *tactoRing* to a pre-specified targets. The user can then disambiguate, eyes-free, among different callers or notifications without interrupting their primary activities. In Figure 10.b dragging motions on the ring are mapped to quantities. We developed an application that simulate a card payment system: when a debit card (with an RFID) is placed on a reader, the user is notified of how much money is left on the card. For example, the tactor movement to the target location at 45° means that 25% of the initial budget is still available on the card, while the movement to location 180° signifies that 50% of the

money available was spent. Also, in this application the information is mapped to locations on the ring and the users can understand them through eyes-free interaction.

Another possible class of applications works by conveying exact directions on the ring through tactile feedback. For example, Figure 11.a is a prototype of a car navigation interface, where street directions (left, right, forward, turn back) can be signaled on the hand, without the need for additional visual information. Finally, Figure 11.b presents an input-output ring: using a set of four capacitive electrodes placed around the *tactoRing* we are able to discern touch input in the four cardinal locations and transmit those locations to a remote user, who is also wearing the *tactoRing*. This application is open-ended and leads to a variety of scenarios. For example, the *tactoRing* platform could form an implicit and effective tele-communications tool for remote users to communicate through touch input and receive messages as tactile stimuli on the ring.

CONCLUSIONS

In this paper we presented *tactoRing*, the first example of a wearable skin-drag display capable of encoding discrete locations around the finger. We presented the description of a smart ring prototype with a movable tactor which rotates around the finger, and presented evidence of accuracy with users engaged in targeting task with up to eight different locations. Based on the performance in the first study, we then designed two interaction techniques (*DoublePoint* and *VirtualPoint*) that exploit the ability of humans to distinguish dragging motion on the skin (motion excites more skin receptors than static contact). With a second study we demonstrated that both techniques achieve higher results than absolute targeting of static locations. Finally, we presented a set of applications to showcase how skin-dragging cues, single or sequential, can be used to encode complex information without the need of additional visual feedback.

This work also has several limitations and possible areas of improvement. The current hardware is wearable but bulky and power-hungry due to the motor. We reckon that smaller and more efficient motors could be employed. In addition, we acknowledge that the material choice for both the ring body and the tactor (e.g., rigid PLA and plastic vs. elastic material or rubber) could impact performance and perception thresholds for dragging. So further investigation is necessary to determine the effects of materials. We also acknowledge that our results are strongly linked with the stimulated surface area of the finger's proximal phalanx, and different perception thresholds may be expected on other body parts, with their unique density of skin receptors. Therefore, we feel it is important to investigate tactile dragging perception on other continuous non-planar surfaces, such as the wrist, forearms [23], legs and the neck by modifying the form-factor of the interfaces (e.g., bracelets, necklaces).

Possible future directions include: developing smaller hardware capable of adapting to different surface areas; testing tactors of different shapes, size and materials; and, further studies to gauge perception performance. Following Ion [13], we are interested in comparing directional and compound dragging cues for encoding with one-dimensional motions, with the performance of *DoublePoint* and *VirtualPoint* techniques with revised distinctive drag-motion sets. Moreover, similarly to Roument et al. [28], we are interested in differences of perception for dragging motions in static vs dynamic positions (e.g., walking). Also, following the prominent work on tactons [3], we are interested in exploring more complex dragging-pattern encoding using temporal elements, direction and speed of motion, and even sequences of motions.

ACKNOLEDGEMENTS

This paper was supported by the MSIP, Korea, under the G-ITRC support program (IITP-2016-R6812-16-0001) supervised by the IITP.

REFERENCES

1. Daniel Ashbrook, Patrick Baudisch, and Sean White. 2011. Nenya: subtle and eyes-free mobile input with a magnetically-tracked finger ring. In Proceedings of the SIGCHI Conference on Human Factors in Computing Systems (CHI '11). ACM, New York, NY, USA, 2043-2046.
2. Karlin Bark, Jason W. Wheeler, Sunthar Premakumar, Mark R. Cutkosky. (2008). Comparison of skin stretch and vibrotactile stimulation for feedback of proprioceptive information. In Proc. HAPTICS'08, 71–78.
3. Stephen Brewster and Lorna M. Brown. 2004. Tactons: structured tactile messages for non-visual information display. In Proceedings of the fifth conference on Australasian user interface - Volume 28 (AUIC '04).
4. Nathaniel A. Caswell, Ryan T. Yardley, Markus N. Montandon, William R. Provancher. 2012. Design of a forearm-mounted directional skin stretch device. In Proc. HAPTICS'12, 365–370.
5. Liwei Chan, Rong-Hao Liang, Ming-Chang Tsai, Kai-Yin Cheng, Chao-Huai Su, Mike Y. Chen, Wen-Huang Cheng, and Bing-Yu Chen. 2013. FingerPad: private and subtle interaction using fingertips. In Proceedings of the 26th annual ACM symposium on User interface software and technology (UIST '13). ACM, New York, NY, USA, 255-260.
6. Ke-Yu Chen, Kent Lyons, Sean White, and Shwetak Patel. 2013. uTrack: 3D input using two magnetic sensors. In Proceedings of the 26th annual ACM symposium on User interface software and technology (UIST '13). ACM, New York, NY, USA, 237-244.
7. Francesco Chinello, Monica Malvezz, Claudio Pacchierotti, and Domenico Prattichizzo. A three DoFs wearable tactile display for exploration and manipulation of virtual objects. 2012. In

Proceedings 2012 IEEE Haptics Symposium (HAPTICS). IEEE. p. 71-76.

8. Brian T. Gleeson, Scott K. Horschel, and William R. Provancher. Communication of direction through lateral skin stretch at the fingertip. In Proceedings of EuroHaptics conference, 2009 and Symposium on Haptic Interfaces for Virtual Environment and Teleoperator Systems. World Haptics 2009. Third Joint. IEEE, 2009. p. 172-177.
9. Ashley L. Guinan, Nicholas C. Hornbaker, Markus N. Montandon, Andrew J. Doxon, and William R. Provancher. Back-to-back skin stretch feedback for communicating five degree-of-freedom direction cues. In Proceedings of World Haptics Conference (WHC), 2013. IEEE, 2013. p. 13-18.
10. Michitaka Hirose, and Tomohiro Amemiya. Wearable finger-braille interface for navigation of deaf-blind in ubiquitous barrier-free space. Proceedings of the HCI International. Vol. 4. 2003.
11. Chih-Pin Hsiao, Richard Li, Xinyan Yan, and Ellen Yi-Luen Do. 2015. Tactile Teacher: Sensing Finger Tapping in Piano Playing. In Proceedings of the Ninth International Conference on Tangible, Embedded, and Embodied Interaction (TEI '15). ACM, New York, NY, USA, 257-260.
12. Meng-Ju Hsieh, Rong-Hao Liang, and Bing-Yu Chen. 2016. NailTactors: eyes-free spatial output using a nail-mounted tactor array. In Proceedings of the 18th International Conference on Human-Computer Interaction with Mobile Devices and Services (MobileHCI '16). ACM, New York, NY, USA, 29-34.
13. Alexandra Ion, Edward Jay Wang, and Patrick Baudisch. 2015. Skin Drag Displays: Dragging a Physical Tactor across the User's Skin Produces a Stronger Tactile Stimulus than Vibrotactile. In Proceedings of the 33rd Annual ACM Conference on Human Factors in Computing Systems (CHI '15). ACM, New York, NY, USA, 2501-2504.
14. Lynette A. Jones and Susan j. Lederman. 2006. Human Hand Function. Oxford University Press.
15. Haruhisa Kawasaki, Yasuhiko Doi, Shinya Koide, Takahiro Endo, and Tetsuya Mouri. Hand haptic interface incorporating 1D finger pad and 3D fingertip force display devices. 2010. In Proceedings 2010 IEEE International Symposium on Industrial Electronics. IEEE. p. 1869-1874.
16. Hamed Ketabdar, Peyman Moghadam, and Mehran Roshandel. 2012. Pingu: A new miniature wearable device for ubiquitous computing environments. InProceedings Complex, Intelligent and Software Intensive Systems (CISIS).
17. Sugarragchaa Khurelbaatar, Yuriko Nakai, Ryuta Okazaki, Vibol Yem, and Hiroyuki Kajimoto. 2016. Tactile Presentation to the Back of a Smartphone with Simultaneous Screen Operation. In Proceedings of the 2016 CHI Conference on Human Factors in Computing Systems (CHI '16).
18. Wolf Kienzle and Ken Hinckley. 2014. LightRing: always-available 2D input on any surface. In Proceedings of the 27th annual ACM symposium on User interface software and technology (UIST '14). ACM, New York, NY, USA, 157-160.
19. Hwan Kim, Minhwan Kim, and Woohun Lee. 2016. HapThimble: A Wearable Haptic Device towards Usable Virtual Touch Screen. In Proceedings of the 2016 CHI Conference on Human Factors in Computing Systems (CHI '16). ACM, New York, NY, USA, 3694-3705.
20. Kevin A. Li, Patrick Baudisch, William G. Griswold, and James D. Hollan. 2008. Tapping and rubbing: exploring new dimensions of tactile feedback with voice coil motors. In Proceedings of the 21st annual ACM symposium on User interface software and technology (UIST '08).
21. Stefan Marti and Chris Schmandt. 2005. Giving the caller the finger: collaborative responsibility for cellphone interruptions. In CHI '05 Extended Abstracts on Human Factors in Computing Systems (CHI EA '05). ACM, New York, NY, USA, 1633-1636.
22. Cameron S. Miner, Denise M. Chan, and Christopher Campbell. 2001. Digital jewelry: wearable technology for everyday life. In CHI '01 Extended Abstracts on Human Factors in Computing Systems (CHI EA '01). ACM, New York, NY, USA, 45-46.
23. Ulf Norrsell, Hakan Olausson. 1994. Spatial cues serving the tactile directional sensibility of the human forearm. Journal of Physiology, 478 (3), 533-540.
24. Masa Ogata, Yuta Sugiura, Hirotaka Osawa, and Michita Imai. 2012. iRing: intelligent ring using infrared reflection. In Proceedings of the 25th annual ACM symposium on User interface software and technology (UIST '12). ACM, New York, NY, USA, 131-136.
25. Gilang Andi Pradana, Adrian David Cheok, Masahiko Inami, Jordan Tewell, and Yongsoon Choi. 2014. Emotional priming of mobile text messages with ring-shaped wearable device using color lighting and tactile expressions. In Proceedings of the 5th Augmented Human International Conference (AH '14). ACM, New York, NY, USA, Article 14 , 8 pages.
26. William R. Provancher, and Nicholas D. Sylvester. Fingerpad skin stretch increases the perception of virtual friction. In Proceedings of IEEE Transactions on Haptics, 2009, 2.4: 212-223.

27. Zhan Fan Quek, Samuel B. Schorr, Ilana Nisky, William R. Provancher, and Allison M. Okamura. Sensory substitution using 3-degree-of-freedom tangential and normal skin deformation feedback. In Proceedings of 2014 IEEE Haptics Symposium (HAPTICS). IEEE, 2014. p. 27-33.
28. Thijs Roumen, Simon T. Perrault, and Shengdong Zhao. 2015. NotiRing: A Comparative Study of Notification Channels for Wearable Interactive Rings. In Proceedings of the 33rd Annual ACM Conference on Human Factors in Computing Systems (CHI '15). ACM, New York, NY, USA, 2497-2500.
29. Roy Shilkrot, Jochen Huber, Jürgen Steimle, Suranga Nanayakkara, and Pattie Maes. 2015. Digital Digits: A Comprehensive Survey of Finger Augmentation Devices. ACM Comput. Surv. 48, 2, Article 30 (November 2015), 29 pages.
30. Chao-Huai Su, Liwei Chan, Chien-Ting Weng, Rong-Hao Liang, Kai-Yin Cheng, and Bing-Yu Chen. 2013. NailDisplay: bringing an always available visual display to fingertips. In Proceedings of the SIGCHI Conference on Human Factors in Computing Systems (CHI '13). ACM, New York, NY, USA, 1461-1464.
31. Hong Z. Tan, Nathaniel I. Durlach, William M. Rabinowitz, Charlotte M. Reed. 1997. Reception of morse code through motional, vibrotactile and auditory stimulation. Perception & Psychophysics 59, 7.
32. Leslie G. Valiant. 1979. The complexity of enumeration and reliability problems. SIAM Journal on Computing, 8 (3), 410-421.
33. Åke B. Vallbo, and Roland S. Johansson. Properties of cutaneous mechanoreceptors in the human hand related to touch sensation. Hum Neurobiol 3.1 (1984): 3-14.
34. Douglas B. West. 1996. Introduction to graph theory. Prentice Hall.
35. Xing-Dong Yang, Tovi Grossman, Daniel Wigdor, and George Fitzmaurice. 2012. Magic finger: always-available input through finger instrumentation. In Proceedings of the 25th annual ACM symposium on User interface software and technology (UIST '12). ACM, New York, NY, USA, 147-156.
36. Vibol Yem, Ryuta Okazaki, and Hiroyuki Kajimoto. 2016. FinGAR: combination of electrical and mechanical stimulation for high-fidelity tactile presentation. In ACM SIGGRAPH 2016 Emerging Technologies (SIGGRAPH '16). ACM, New York, NY, USA, Article 7, 2 pages.